Available online at www.sciencedirect.com
SCIENCE DIRECT®
Materials Science in Semiconductor Processing 8 (2005) 622–629
MATERIALS SCIENCE IN SEMICONDUCTOR PROCESSING

A comparative molecular dynamics study of copper trench fill properties between Ta and Ti barrier layers

J.Y. Yang[a,*], R.T. Hong[b], M.J. Huang[b]

[a]*Institute of Applied Mechanics, National Taiwan University, No. 1, Section 4, Roosevelt Road, Taipei, 10764, Taiwan*
[b]*Department of Mechanical Engineering, National Taiwan University, No. 1, Section 4, Roosevelt Road, Taipei, 10764, Taiwan*

Available online 27 March 2006

Abstract

The copper atoms deposition on tantalum diffusion barrier layer in a damascene process was studied using molecular dynamics simulation with the embedded atom method (EAM) as interaction potential for the present alloy metal system which is based on invariance-preserving alloy model. The present results are discussed in terms of void formation, coverage percentage and alloy fraction. The effects of different process parameters on the trench-filling morphologies and microstructures including incident energies of depositing atoms and substrate temperatures were investigated. Comparing with Ti diffusion barrier under the same process parameters, it is found that due to better thermal stability that significant improvement in coverage percentage can be obtained using the tantalum barrier layer, especially at high incident energies and high substrate temperatures.

Keywords: Tantalum barrier layer; Embedded atom method; Damascene process; Molecular dynamics simulation

1. Introduction

Interconnects are used to connect devices electrically in integrated circuits. As feature sizes decrease below a quarter micron, the scaling of interconnects poses several serious metallization problems such as high RC and electromigration resistance. To improve the electrical properties problems, copper (Cu) is used instead of aluminum for interconnects. A review on the overall requirements for diffusion barrier layers has been given by Kattelus and Nicolet [1]. There are many refractory materials and compounds that are used as barrier layer in Cu interconnect [2–4]. Ta is thermodynamically stable with respect to Cu and Ta is almost completely immiscible up to their melting point and do not react with Cu to produce any compounds. Ta has good adhesion to both Cu and dielectrics and is known to be more effective than Ti as a diffusion barrier in Cu metallization. We shall investigate the effects of using both Ta and Ti barrier layers in Cu Damascene trench filling with physical vapor deposition (PVD). There are many simulation approaches have been explored in deposition simulation [5–9].

In this work, the molecular dynamics simulation is used to study the *trench filling* and microstructures for depositing Cu into Ta diffusion barrier layer in Damascene process. The processes parameters considered including incident energies of depositing atoms and substrate temperatures and

*Corresponding author.
E-mail address: yangjy@spring.iam.ntu.edu.tw (J.Y. Yang).

1369-8001/$ - see front matter © 2006 Elsevier Ltd. All rights reserved.
doi:10.1016/j.mssp.2006.02.001

their effects on the trench-filling morphologies, coverage percentages, and alloy fraction are studied in detail for Ta barrier layer. We also compare the microstructure differences and trench filling between Ta and Ti barrier layers in Cu Damascene process. This paper is a sequel to [10] and we will constantly refer to [10] for the results using Ti barrier layer without duplicating them here.

2. Computational model

The model for trench filling with MD simulation includes a trench model, a deposition model, and a potential model. The trench model is the same as described in previous work [10]. The computational domain is $169.74 \times 25.25 \times 225.30$ Å and the aspect ratio of trench is 1 with the depth of trench 10 nm. The atoms of barrier layer for Ta are arranged by basic cubic crystal (bcc) structure with surface (1 0 0) for Ta barrier layer initially and the single-crystal arrangement hcp and surface (0 0 0 1) is used for Ti barrier layer. Both barrier layers have no grain boundary and amorphous crystal arrangement before simulation. In deposition model, we prepare the incident atoms to add into system before simulation. The positions of incident Cu atoms are arranged randomly in x, y directions. The positions of incident atoms in z direction are started from the height of simulation domain and the gap (Δz) between sequential incident atoms is determined by the depositing rate and the magnitude of velocity is determined by incident energies. As the simulation is advancing, we add nearly 6 incident Cu atoms into the system per 1 ps. The angular distributions deposition is used for incident atoms and are assumed to be confined within the range of zenith angle, from -5° to $+5^\circ$, and the range of azimuth angle, from 0° to 360°. Since only the short-range forces were considered in this work, we did not consider reflected atoms and the resputter atoms which include Cu adatoms and tantalum (titanium) atoms on barrier layer. They are removed from the system when they are far (larger than cutoff-range 6 Å) from the barrier (deposited) layers. We detect free atoms that no longer interact with the substrate by observing force value of every atom. The atoms that have zero force value are labeled as free atoms in our program and these free atoms are removed from the system. As for the interatomic potential model, the embedded atom method (EAM) [11–13] is used which is an isotropic many-body pair-function potential. The total energy acting on each atom is computed from the sum of the local embedded energy and two-body potential as

$$E_{\text{tot}} = \sum_i F(\rho_i) + \frac{1}{2}\sum_i \sum_{j\neq i} \phi_{ij}(r_{ij}), \tag{1}$$

$$\rho_i = \sum_{j\neq i} f(r_{ij}), \tag{2}$$

where E_{tot} is the total internal energy, F is the embedding energy, ρ_i is the local electron density at atom i, $\phi(r_{ij})$ is the pair potential and r_{ij} is the distance between atom i and atom j. A nearest-neighbor analytic form EAM potential is used in this work that *is suitable for* MD simulations has been proposed by Johnson [14]. The analytical forms of EAM have been developed for many metals and have yielded reasonable fits to physical properties [15]. The two-body potential and electron density function as given by Johnson can be written, respectively, as

$$\phi(r) = \frac{A\mathrm{e}^{-\alpha((r/r_{\text{e}})-1)}}{1+((r/r_{\text{e}})-\kappa)^m} - \frac{B\mathrm{e}^{-\beta((r/r_{\text{e}})-1)}}{1+((r/r_{\text{e}})-\lambda)^n}, \tag{3}$$

$$f(r) = \frac{f_{\text{e}}\mathrm{e}^{-\beta((r/r_{\text{e}})-1)}}{1+((r/r_{\text{e}})-\lambda)^n}. \tag{4}$$

The model parameters for Cu, Ti and Ta atoms are listed in Table 1. The embedding energy of the atom i is determined by the local electron density at the position of the atom and the embedding energy is

Table 1
Electron density function and two-body potential parameters for metals of EAM

	r_{e} (Å)	f_{e} (eV/Å)	ρ_{e} (eV/Å)	α	β	A	B	κ	λ	m	n
Cu	2.556	1.554	22.150	7.670	4.091	0.328	0.469	0.431	0.863	20.0	20.0
Ti	2.930	1.860	25.600	8.780	4.680	0.328	0.469	0.431	0.863	20.0	20.0
Ta	2.560	1.550	22.200	8.489	4.528	0.330	0.470	0.430	0.86	20.0	20.0

Table 2
Embedding function parameters for metals of EAM

	η	F_{n0} (eV)	F_{n1} (eV)	F_{n2} (eV)	F_{n3} (eV)	F_0 (eV)	F_1 (eV)	F_2 (eV)	F_3 (eV)
Cu	0.921	−2.176	−0.140	0.286	−1.751	−2.190	0.000	0.703	0.684
Ti	0.560	−3.200	−0.200	0.680	−2.320	−3.220	0.000	0.610	−0.750
Ta	0.920	−5.104	−0.405	1.113	−3.585	−5.140	0.000	1.640	0.221

determined as [16]

$$F(\rho) = \sum_{i=0}^{3} F_{ni}\left(\frac{\rho}{\rho_n} - 1\right)^i, \quad \rho < \rho_n, \ \ \rho_n = 0.85\rho_e, \tag{5}$$

$$F(\rho) = \sum_{i=0}^{3} F_i\left(\frac{\rho}{\rho_e} - 1\right)^i, \quad \rho_n \leqslant \rho < \rho_0, \ \ \rho_0 = 1.15\rho_e, \tag{6}$$

$$F(\rho) = F_0\left(1 - \ln\left(\frac{\rho}{\rho_e}\right)^\eta\right)\left(\frac{\rho}{\rho_e}\right)^\eta, \quad \rho_0 < \rho, \tag{7}$$

where the parameters in Eqs. (5)–(7) are given in Table 2.

For an alloy model with the EAM, we adopt Johnson's alloy model with EAM which satisfies the condition for transformation of invariance [17] and the alloy two-body potential can be determined as

$$\phi^{ab}(r) = \frac{1}{2}\left[\frac{f^b(r)}{f^a(r)}\phi^{aa}(r) + \frac{f^a(r)}{f^b(r)}\phi^{bb}(r)\right], \tag{8}$$

where ϕ^{ab} is the alloy potential, f is the density function as given by (4) and the superscripts aa and bb stand for monatomic a and monatomic b, respectively.

In MD simulation, the trajectories of atoms are determined by Newton's equation of motion and integrated by the Velocity-Verlet scheme [18], see also [19]. Due to long time calculation in MD simulation, the parallel computation technique is used and implemented with the spatial decomposition method. The whole computational domain is decomposed into several sub-domains with each sub-domain assigned to a processor and the calculation of interaction among neighboring processors communicate spatially. Because the number of simulated atoms in the system are increased as simulation is advancing and the number of atoms of each sub-domain are not uniform. For load balance and computational homogenerity, the size of computational sub-domain is adaptively changed and is depended on the number of atoms of each sub-domain.

3. Results and discussion

We will investigate the influences of incident energy of Cu atom and substrate temperature on the morphology and microstructure of the trench filling. Three incident energies, 1, 3, and 10 eV and three substrate temperatures, 300, 550 and 700 K are considered. The results are demonstrated in three-dimensional plots at various stages of deposition to help explaining and understanding the trench-filling process. In following figures, we use the white balls to denote depositing Cu atoms which have not interacted with the substrate yet and the dim grey balls are deposited Cu atoms.

3.1. Effect of incident energy

We consider the effects of incident energy on the morphology of the trench filling by varying the incident energies and keeping the substrate temperature constant at 300 K. In the case of lower incident energies, the coverage percentage and microstructure are similar to [10] and will be not discussed here. In the case of 10 eV, the Cu adatoms have more mobility when the Cu adatoms get more energy from the depositing Cu atoms constantly. Meanwhile, the Cu adatoms are more difficult to diffuse into the barrier layer because the Ta has deeper potential well. Due to above reasons, the distribution of deposited Cu atoms are more flatten at early stage as shown in Fig. 1(a). As time evolves, the deposited cluster on trench opening merges with that of bottom before merging with other deposited cluster on trench opening that make more Cu incident atoms passing into trench as shown in Fig. 1(b). Due to higher mobility of Cu adatoms, the shadowing effect is reduced such that the coverage percentage is improved significantly for Ta barrier layer and there exists only a small void on right bottom of trench as shown in Fig. 1(c). Next, we investigate the intermixing of Cu and Ta atoms. The interface intermixing is that the positions of Ta atoms are exchanged by deposited Cu

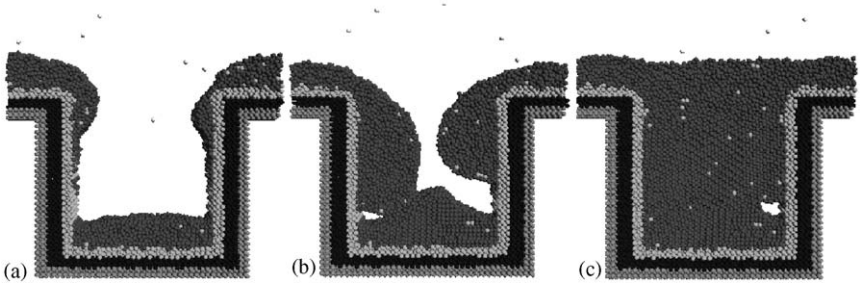

Fig. 1. Snapshots for $E_{atom} = 10\,eV$ and $T_{sub} = 300\,K$. (a) 90 ps, (b) 1980 ps, (c) 3000 ps.

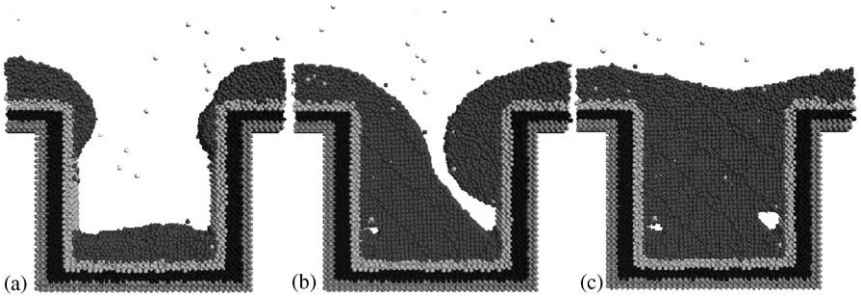

Fig. 2. Snapshots for $E_{atom} = 3\,eV$ and $T_{sub} = 550\,K$. (a) 90 ps, (b) 2300 ps, (c) 2800 ps.

atoms on the interface. This energy-dependent intermixing mechanism has been studied for vapor deposition of metal multilayers by Zhou and Wadley [20]. They found that high incident atom energies would lower interfacial roughness but promote intermixing by an atomistic exchange mechanism. The probability of exchange increases with the adatom energy strongly. The exchange mechanism depends upon the energy barrier at flat surface and edges of substrate. We can find that the intermixing will occur on the trench opening first because the total energy barrier there is less than that of other regions. The intermixing for higher incident energy is more serious than that for lower incident energy due to the local substrate temperature is increased by incident kinetic energy of Cu atoms [21]. In all cases of incident energies, the exchange mechanism is inhibited nearly because of the Ta atom has large cohesive energy to resist the higher energetic Cu deposition.

3.2. Effects of substrate temperature

To investigate the effects of substrate temperature on the filling coverage of the trench and trench-filling morphology, we consider three temperatures, 300, 550, and 700 K while the incident energy is kept at 3 eV. As the substrate temperature elevated to 550 K, due to the higher temperature of Ta film, the deposited Cu atoms gain additional thermal energy from the high temperature Ta atoms and improve their mobility and become more movable when bombarded by subsequently incident Cu atoms. The deposited cluster on the side walls with higher thermal energy will flow further downward along both side walls that the effect of shadowing is reduced and the two bottom corners are better filled, see Fig. 2(a). As there is more space available between the two trenching openings, there are many more Cu atoms can be deposited within the trench. Later, the left cluster touches the bottom bulge first and a small void is formed as shown in Fig. 2(b). At further later time, the other cluster touches the already merged cluster and bottom bulge and another void is formed, as shown in Fig. 2(c). It is interesting to note that there exist several marked texture orientation of deposited Cu atoms (which are making 135° angle with respect to the x-axis) as can be clearly observed in Fig. 2(c). In the case of 700 K, the deposited Cu clusters move downward on both side walls of the trench, thus the shadowing effect is inhibited and there are more depositing Cu atoms will pass through into the trench. The distribution of deposited Cu cluster on the bottom

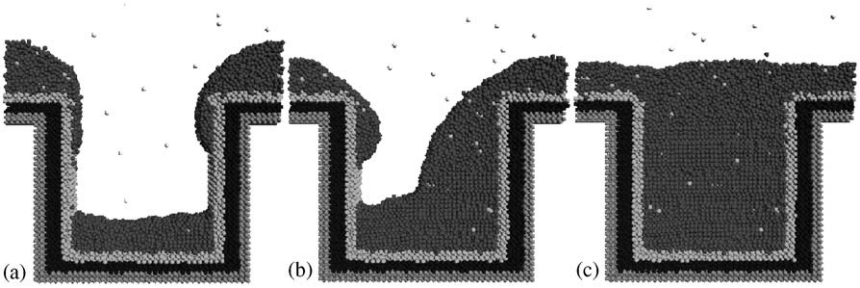

Fig. 3. Snapshots for $E_{atom} = 3\,eV$ and $T_{sub} = 700\,K$. (a) 102 ps, (b) 1740 ps, (c) 2940 ps.

flatten and the Cu atoms are deposited deeply on side walls as shown in Fig. 3(a), such that there is no void formed when the right deposited Cu cluster merges with bottom, as shown in Fig. 3(b). Due to the better distribution of deposited Cu cluster, the Cu atoms fill the trench completely at later stage of simulation, see Fig. 3(c). Although the diffusion coefficient of barrier layer is increased by raising the substrate temperature, the Cu adatoms have difficulty to diffuse into Ta barrier layer because of the immiscibility between the metals Ta and Cu [22]. The deposited Cu cluster will move along the surface of Ta barrier layer. Due to the fact that Ta has better thermal stability in high temperature that the effect of diffusion will be inhibited in case of higher substrate temperature. Therefore, the intermixing between Cu adadoms and Ta substrate is not so serious in the 700 K case. There are damages of Ta barrier on the trench opening and wings (about 7.68 Å thick) caused by the incident Cu atoms and the other regions are retained very well. The trenchfilling is promoted and the size of trapped void is reduced by increasing the substrate temperature. This provides further evidence that an elevated substrate temperature improves the mobility of the deposited Cu atoms and gets better deposition distribution.

3.3. Comparison of coverage percentage

The coverage percentages of trench filling for various cases simulated in this work are shown in Fig. 4, which indicate the effects of the incident atoms energy and the substrate temperature. The coverage percentage is determined as the number of deposited atoms within the trench divided by the number of atoms required for perfect coverage within the trench. At constant 300 K substrate temperature, the coverage percentage is promoted with increasing the incident energy and it is

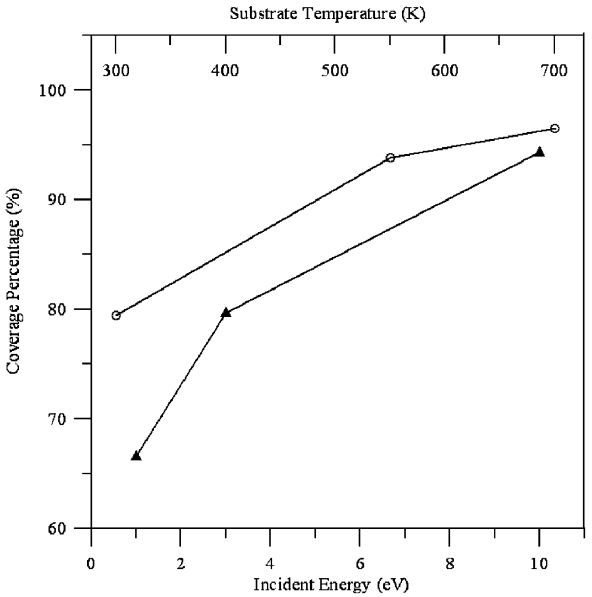

Fig. 4. A comparison of the coverage percentage for different cases. (△) is for various incident energies at constant 300 K and (○) is for various substrate temperatures at constant 3 eV.

promoted from 67.7% at 1 eV to 93.27% at 10 eV. The coverage percentage is poor for the case of 1 eV because that most incident Cu atoms are deposited on the wings and the opening of trench that preventing the Cu atoms from depositing into the trench. The promotion of coverage percentage from 1 to 3 eV is higher than that from 3 to 10 eV which reveals the shadowing effect is more significant for lower incident energies. At constant 3 eV incident energy, the coverage percentage is promoted from 79.7% to about 96.7% with temperature increasing from 300 to 700 K. By increasing the substrate temperature, the fluidity of deposited Cu cluster is increased and it flows along the side walls, thus more Cu atoms can deposit into the trench. The coverage percentage is increased by 14.4% with the

temperature increase from 300 to 550 K but it is just increased by 2.3% from 550 to 700 K. This indicates that the promotion of coverage percentage is not so effective after exceeding certain high substrate temperatures. According to the above results, increasing substrate temperature will improve the coverage percentage more effectively than increasing incident energy of depositing Cu atoms onto Ta-based trench.

3.4. Comparison with Ti barrier layer

We investigate the trench-filling morphology and intermixing of Cu atoms deposition into the trench for Ta and Ti barrier materials under various incident energies and substrate temperatures. The results of Ti-based trench can be found in previous work [10]. First, we investigate the trench filling for various incident energies. In the cases of 1 and 3 eV, there exists no clear difference of coverage percentage between Ta and Ti. However, there exist substantial differences at 10 eV; the value is 93.27% for Ta-based trench and 86.26% for Ti-based trench as shown in Fig. 5. The exchange mechanism depends on the surface energy of substrate. The surface energy of Ta is higher than that of Ti for various temperatures [23,24] and most of surface energy of temperature-dependence stems from surface energy of zero temperature by MD simulation [25]. The exchange of Cu adatoms into Ta barrier layer is inhibited and the deposited Cu cluster moves along the side walls of the trench with subsequent Cu atoms bombardment. Contradictory, the Cu adatoms diffuse into Ti barrier layer and the intermixing cluster of Cu–Ti is formed strongly. The alloy Cu–Ti potential well is deeper than pure Cu metal that the mobility of deposited intermixing cluster is reduced, thus the coverage percentage is reduced due to the fact that a lot of incident Cu atoms are deposited on the trenching opening. Next, we investigate the coverage percentage for various substrate temperatures. The coverage percentages are similar in the case of 300 K. In the case of 550 K, the coverage percentage is 94.24% for Ta-based trench and is higher than 82.67% for Ti-based trench as shown in Fig. 6. There exists marked difference in coverage percentage. As discussed above in terms case of incident energy of Cu, the intermixing cluster will affect the mobility. The Cu adatoms will diffuse more into the barrier layer because of activation energy and surface energy are decreased as increasing substrate temperature. As a result, more energetic Cu adatoms diffuse into Ti barrier during bombardment of Cu atoms constantly at substrate temperature 550 K. Due to the better diffusivity of Ta at higher temperatures, the energetic Cu adatoms are resisted for diffusing into barrier layer. In the case of higher substrate temperature, 700 K, the Ti

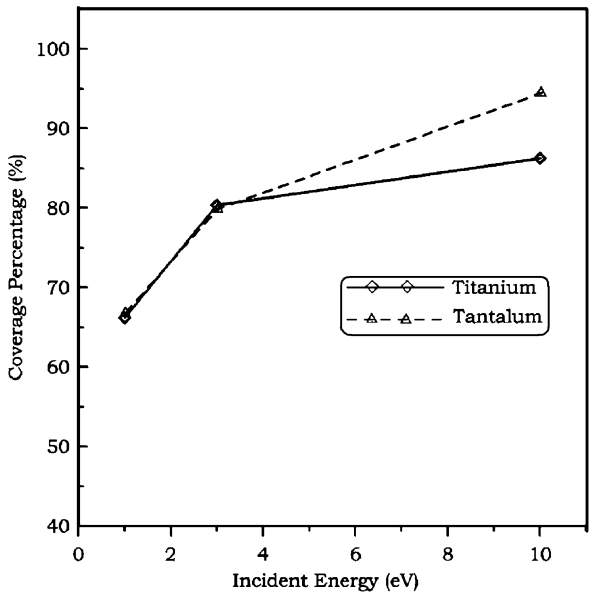

Fig. 5. A comparison of the coverage percentage of barrier materials at constant 300 K.

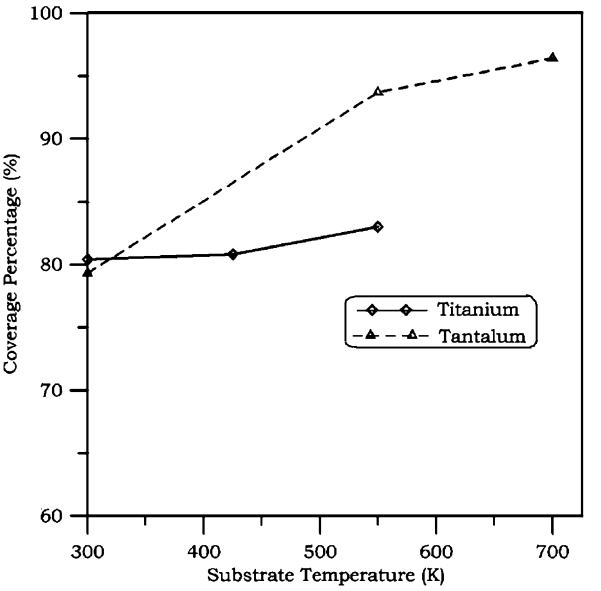

Fig. 6. A comparison of the coverage percentage of barrier materials at constant incident energy 3 eV.

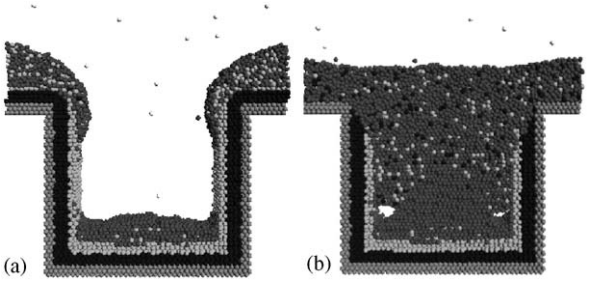

Fig. 7. Snapshots of Ti-based trench for $E_{atom} = 3\,eV$ and $T_{sub} = 700\,K$. (a) 60 ps, (b) 2520 ps.

barrier layer is almost destroyed at early stage (60 ps) of simulation that means the deposited Cu adatoms will diffuse into the barrier layer due to the higher value of diffusion coefficient and low surface energy. The thermal stability of Ti is low as compared with that of Ta and the exchange mechanism will occur strongly for Cu adatoms to penetrate Ti barrier layer as depicted in Fig. 7(a). At later stage, the intermixing between Cu adatoms and Ti barrier layer interface occur constantly by an atomistic exchange mechanism, thus the Ti barrier layer is damaged seriously as shown in Fig. 7(b). Fig. 7(b) reveals that Cu adatoms penetrate into dielectric materials from the wings and corners of trench. Due to better interfacial behavior between immiscible Cu and Ta, the boundary of interface is clean at early stage as shown in Fig. 3(a). The deposited Cu cluster has more difficulty to diffuse into Ta barrier which is in good agreement with previous works [26,27]. Thus, dielectric substrate has stronger diffusion protection in Cu interconnect.

4. Conclusion

Based on the present parametric study and our previous work on Ti barrier layer [10], it is possible to summarize the conclusions as following:

(i) The coverage percentage of trench filling can be promoted effectively by increasing the energy of incident atoms and the temperature of substrate through incident atoms punch effect and increasing mobility. To increase the coverage percentage, the effect of increasing substrate temperature is better than that raising the incident Cu energy. Also, comparing with Ti barrier, the improvement of coverage percentage at higher incident energy and higher substrate temperature is significant when Ta barrier is used.

(ii) By examining morphologies of microstructures simulated in this work, the intermixing of Cu deposited cluster with Ta barrier layer is significantly inhibited compared to that using Ti barrier layer and the fraction of alloy formation of Cu/Ta is markedly reduced in sputter depositing Cu interconnect. The boundary between deposited Cu cluster and Ta barrier is discrete and very little intermixing had occurred at the interfaces. This provides further evidence that Ta is immiscible with Cu atom. The performance is improved by using Ta barrier instead of Ti barrier.

(iii) The thickness of barrier layer required for proper functioning can be reduced for Ta barrier as compared with using Ti barrier layer when higher substrate temperature is used for better trench filling. Thus, thinner thickness of barrier layer can be used to yield better performance in Cu interconnects.

(iv) For the case of incident energy 3 eV and substrate temperature 550 K, it is found that peculiar texture orientation lines in the deposited Cu atoms are observed when Ta barrier layer is used. We did not find such phenomena in our previous work using Ti barrier layer. Further study on this aspect is warranted.

Acknowledgments

The authors would like to thank the reviewers for many constructive comments. They also acknowledge the support of the National Center for High-Performance Computing in providing resources under the national project "Knowledge Innovation National Grid" in Taiwan. This work was done under the auspices of National Science Council, TAIWAN through grant (NSC 93-2210-E002-006).

References

[1] Kattelus HP, Nicolet MA. In: Gupta D, Ho PS, editors. Diffusion phenomena in thin films and microelectronic materials. Park Ridge, NJ: Noyes; 1989. p. 432.
[2] Holloway K, Fryer PM. Appl Phys Lett 1990;57(17):1736–8.
[3] Castoldi L, Visalli G, Morin S, Ferrari P, Alberici S, Ottaviani G, et al. Microelect Eng 2004;76:153–9.
[4] Kaloyeros AE, Eisenbraun E. Annu Rev Mater Sci 2000;30:363–85.
[5] Hamaguchi S, Rossnagel M. J Vac Sci Technol B 1995; 13(2):183–91.

[6] Adalsteinsson D, Sethian JA. J Comput Phys 1995;120(1):348–66.
[7] Huang CH, Glimer GH, Rubia TD. J Appl Phys 1998;84(7):3636–49.
[8] Yang YG, Zhou XW, Johnson RA. J Vac Sci Technol B 2002;20(2):622–30.
[9] Zhou XW, Johnson RA, Wadley HNG. Acta Mater 1997;45(4):1513–24.
[10] Hong RT, Huang MJ, Yang JY. Mater Sci Semicond Proc 2005;8(5):587–601.
[11] Stott MJ, Zaremba JE. Phys Rev B 1980;22(4):156–83.
[12] Daw MS, Baskes MI. Phys Rev Lett 1983;50(17):1285–8.
[13] Daw MS, Baskes MI. Phys Rev B 1984;29(12):6443–53.
[14] Johnson RA. Phys Rev B 1988;37(8):3924–31.
[15] Johnson RA, Oh DJ. J Mater Res 1989;4:1195–201.
[16] Wadley HNG, Zhou X, Johnson RA, Neurock M. Prog Mater Sci 2001;46(3–4):329–77.
[17] Johnson RA. Phys Rev B 1989;39(17):12554–99.
[18] Verlet L. Phys Rev 1967;159(1):98–103.
[19] Rapaport DC. The art of molecular dynamics simulation. New York: Cambridge University Press; 1996.
[20] Zhou XW, Wadley HNG. J Appl Phys 1998;84(4):2301–15.
[21] Zhou XW, Wadley HNG. Surf Sci 1999;431:42–57.
[22] Subramanian PR, Laughlin DE. Bull Alloy Phase Diagrams 1989;10:652–86.
[23] Vitos L, Ruban AV, Skriver HL, Kollar J. Surf Sci 1998;411:186–202.
[24] Alonso JA, March NH. Electrons in metals and alloys. London: Academic Press; 1989.
[25] Garruchet S, Politano O, Salazar JM, Montesin T. Surf Sci 2005;586:15–24.
[26] Kong LT, Gong HR, Lai WS, Liu BX. J Phys Soc Jpn 2003;72(1):5–8.
[27] Ono H, Nakano N, Ohta T. Appl Phys Lett 1994;64(12):1511–3.